The absence of ABCD2 sensitizes mice to disruptions in lipid metabolism by dietary erucic acid[S]

Jingjing Liu,* Shuang Liang,* Xiaoxi Liu,* J. Andrew Brown,* Kylie E. Newman,* Manjula Sunkara,[†] Andrew J. Morris,[†,§] Saloni Bhatnagar, Xiangan Li,[†,**] Aurora Pujol,[††] and Gregory A. Graf[1,*,†,§]**

Department of Pharmaceutical Sciences,* Cardiovascular Research Center,[†] Graduate Center for Nutritional Sciences,[§] Kentucky Pediatric Research Institute,** University of Kentucky, Lexington, KY; and Neurometabolic Diseases Laboratory and Institut de Neuropatologia,[††] Institut d'Investigació Biomèdica de Bellvitge (IDIBELL), Catalan Institution of Research and Advanced Studies (ICREA), Barcelona, Spain, and Center for Biomedical Research on Rare Diseases (CIBERER), Spain

Abstract ABCD2 (D2) is a peroxisomal transporter that is highly abundant in adipose tissue and promotes the oxidation of long-chain MUFA. Erucic acid (EA, 22:1ω9) reduces very long chain saturated fatty acids in patients with X-linked adrenoleukodystrophy but promotes dyslipidemia and dilated cardiomyopathy in rats. To determine the role of D2 in the metabolism of EA, we challenged wild-type and D2 deficient mice (D2 KO) with an enriched EA diet. In D2 KO mice, dietary EA resulted in the rapid expansion of adipose tissue, adipocyte hypertrophy, hepatic steatosis, and the loss of glycemic control. However, D2 had no impact on the development of obesity phenotypes in two models of diet-induced obesity. Although there was a significant increase in EA in liver of D2 KO mice, it constituted less than 2% of all fatty acids. Metabolites of EA (20:1, 18:1, and 16:1) were elevated, particularly 18:1, which accounted for 50% of all fatty acids. These data indicate that the failure to metabolize EA in adipose results in hepatic metabolism of EA, disruption of the fatty acid profile, and the development of obesity and reveal an essential role for D2 in the protection from dietary EA.—Liu, J., S. Liang, X. Liu, J. A. Brown, K. E. Newman, M. Sunkara, A. J. Morris, S. Bhatnagar, X. Li, A. Pujol, and G. A. Graf. **The absence of ABCD2 sensitizes mice to disruptions in lipid metabolism by dietary erucic acid. *J. Lipid Res.* 2012.** 53: **1071–1079.**

Supplementary key words peroxisome • adrenoleukodystrophy • Lorenzo's Oil • insulin resistance • fatty liver • adipose • adipocyte

Peroxisomes are essential for β-oxidation of very long chain fatty acids (VLCFAs) and α-oxidation of branched chain fatty acids (1). However, peroxisomal fatty acid oxidation is incomplete, requiring chain-shortened fatty acyl-CoAs to be shuttled out of peroxisomes and into mitochondria for complete oxidation. Peroxisomes are also required for anabolic lipid metabolism, including the synthesis of ether lipids and some PUFAs. The endogenous synthesis of docosapentaenoic acid (22:5ω6) and docosahexaenoic acid (C22:6ω3, DHA) begins with the essential fatty acids linoleate (9,12-18:2) and linolenate (9,12,15-18:3), respectively (2). Due to the limited types of desaturases in mammals (Δ5, Δ6, and Δ9), elongation and desaturation in the endoplasmic reticulum generates 6,9,12,15,18,21-24:6 and 6,9,12,15,18-24:5, both of which must be transported into peroxisomes and undergo one round of β-oxidation to yield 22 carbon PUFAs (1, 3). A second round of peroxisomal oxidation of yields arachidonic acid (20:4ω6, AA) and eicosapentanoic acid (20:5ω3), but peroxisomal oxidation is not essential for the synthesis of these lipids.

The entry of fatty acids into peroxisomes is thought to be dependent upon their esterification by a peroxisomal acyl-CoA synthetase followed by their transmembrane transport by members of the D-subfamily of ABC transporters (4, 5). Among the four members of this subfamily, only ABCD1 (D1) has been associated with human disease,

This work was funded by grants from the National Institute of Health (Graf: R01DK077632 and_R01DK080874) and by grants from the National Center for Research Resources (5P20RR021954-05) and the National Institute of General Medical Sciences (8 P20 GM103527-05, R01GM50388-19) from the National Institutes of Health. Its contents are solely the responsibility of the authors and do not necessarily represent the official views of the National Institutes of Health or other granting agencies.

Manuscript received 31 October 2011 and in revised form 12 March 2012.

Published, JLR Papers in Press, April 6, 2012
DOI 10.1194/jlr.M022160

Copyright © 2012 by the American Society for Biochemistry and Molecular Biology, Inc.

Abbreviations: AA, arachidonic acid; ACC1, acetyl-CoA carboxylase; ALD, X-linked adrenoleukodystrophy; ChREBP, carbohydrate response element binding protein; D1, ABCD1; D2, ABCD2; D2 KO, D2 deficient; DHA, docosahexanoic acid; EA, erucic acid; ELOVL5, fatty acid elongase 5; HF, high fat; INSIG1, insulin-induced gene-1; INSIG2, insulin-induced gene-2; LF, low fat; LXR, liver X receptor; PPAR, peroxisome proliferator activated receptor; SCD1, stearoyl CoA-desaturase; SFA, saturated fatty acid; SREBP1, sterol receptor binding element protein-1; TG, triglycerides; UCP, uncoupling protein; VLCFA, very long chain saturated fatty acid.

[1]To whom correspondence should be addressed.
e-mail Gregory.Graf@uky.edu

[S] The online version of this article (available at http://www.jlr.org) contains supplementary data in the form of three tables and six figures.

X-linked adrenoleukodystrophy (ALD). ALD is a pleiotropic disorder characterized by the accumulation of VLCFAs in plasma and tissues that presents with varying neurological, adrenocortical, and Leydig cell deficiencies (6, 7). The closest paralog of D1 is D2, which shares greater than 60% amino acid identity in humans and mice and at least some overlapping function in vitro and in vivo (8–12). Although direct evidence for transmembrane transport of fatty acyl-CoA substrates is lacking, human D1 and D2 transgenes have been shown to rescue growth in oleate-containing media and to promote the oxidation of distinct subsets of fatty acids in yeast lacking endogenous peroxisomal fatty acyl-CoA transporters (13, 14). In this system, D2 was most active toward the 22-carbon saturated fatty acid and 22- and 24-carbon PUFAs (14).

Whereas D1 is constitutively expressed in many tissues, D2 is more restricted and dynamically regulated by transcription factors involved in lipogenesis, fatty acid oxidation, and cholesterol elimination. D2 mRNA and protein have been detected in brain, liver, lung, adrenal gland, and skeletal muscle but are most abundant in adipose tissue (9, 15). Within adipose, D2 is restricted to adipocytes and is up-regulated during adipogenesis, presumably by the lipogenic transcription factor sterol receptor element binding protein 1 (SREBP1) (15, 16). Conversely, the expression of D2 is relatively low in liver, but is up-regulated by fasting and peroxisome proliferator activated receptor (PPAR) α agonists (9). Hepatic expression of D2 is suppressed by the liver X receptor (LXR), suggesting a role for D2 in cholesterol metabolism (16). However, the functional significance of this observation is unclear and has not been investigated.

Despite its regulation by transcriptional factors essential for lipid homeostasis in liver and adipose, the physiological role for D2 in lipid metabolism remains largely unknown. The absence of D2 results in a modest accumulation of VLCFAs in liver after feeding with a diet enriched in saturated fat and after prolonged fasting, but these differences did not result in overt metabolic phenotypes, nor did they affect the expression of key metabolic enzymes (12). Similarly, there is no apparent adipose dysfunction, and fatty acid profiles in adipose tissue were largely unaffected in D2 deficient mice (15). As in liver, adrenal, and neural tissues, there was a modest accumulation of 22- and 24-carbon saturated fatty acids (SFAs) and MUFAs. When acutely challenged with a diet enriched in erucic acid (EA) (22:1ω-9), there was a gene-dosage dependent increase in the levels in adipose and plasma (15).

EA is abundant in native cultivars of rapeseed (*Brassica napus*) and is used clinically in combination with oleic acid to reduce plasma levels of VLCFA in patients with ALD due to its ability to inhibit the elongation of SFAs (6). However, it is also associated with a transient lipidosis, dyslipidemia, and the development of dilated cardiomyopathy in rats, effects not observed in mice and opposed by treatment with the PPARα agonist clofibrate (17).

We hypothesized that the absence of D2 would sensitize mice to disturbances in lipid metabolism by dietary EA. Our results indicate that in the absence of D2, dietary EA promotes obesity, insulin resistance, and steatosis. However, the absence of D2 had no impact on the development of obesity phenotypes when challenged with a high-fat (HF) diet or when crossed with leptin-deficient (ob/ob) mice. Although adipose tissue is greatly expanded after EA feeding, the lipid profile is only marginally affected with little accumulation of EA. Although there is a significant increase in EA in liver, it constitutes less than 2% of the total fatty acid pool. Conversely, hepatic SFA and MUFA content are elevated by 2- and 3-fold, respectively. These data suggest that in the absence of D2, peroxisomal metabolism of EA proceeds efficiently in the liver but that EA metabolites disrupt hepatic lipid metabolism, resulting in obesity, insulin resistance, and steatosis.

EXPERIMENTAL PROCEDURES

Animal husbandry

Mice harboring the mutant *Abcd2* allele are maintained on the C57BL/6J background as heterozygotes. Strain refreshing is conducted every five generations using C57BL6/J females obtained from The Jackson Laboratory (Bar Harbor, ME). Genotyping experiments to differentiate *Abcd2*-deficient (D2 KO) from heterozygous and wild-type mice were conducted as previously described (18). Animals were housed in individually ventilated cages in a temperature-controlled room with 14:10 light:dark cycle and provided with enrichment in the form of acrylic huts and nesting material. All mice were maintained on standard rodent chow (Harlan Teklad 2014S) until initiation of experiments. All animal procedures conformed to PHS policies for humane care and use of laboratory animals and were approved by the institutional animal care and use committee at the University of Kentucky.

The EA-enriched diet was custom formulated to contain levels of EA found in native rapeseed oil and contained 21.6% total energy from fat (Research Diets, New Brunswick, NJ) (Supplementary Tables I and II). EA accounted for 55.6% of total fatty acids as determined by GC-MS. The diet was stored at 4°C, provided ad libitum, and replaced twice weekly to limit oxidation. Diets were initiated at 8 weeks of age and continued until termination of the experiment after 8 weeks of feeding (n = 7). A second cohort of wild-type and D2 KO littermates were analyzed for the development of obesity phenotypes after low fat (LF) (10% kCal, Research Diets #D12450B, n = 10) or HF (45% kCal, Research Diets #D12451, n = 13 wt, 8 D2 KO) diets. Diets were initiated at 8 weeks of age. Mice were monitored weekly for weight gain and monthly for body composition. Mice were euthanized at 24 weeks (16 weeks on diet). D2 KO mice were also crossed to a leptin-deficient strain (Lep^{ob}, Strain #000632; The Jackson Laboratory), maintained on standard rodent chow, and analyzed at 8, 12, and 16 weeks of age (n = 11 ob/ob; n = 8 ob/ob D2 KO).

Body composition was determined by EchoMRI at the initiation of the feeding period and the day before the termination of the study. During week 7, fasting blood glucose levels were measured using a standard glucometer from a drop of blood obtained by tail-vein prick after a 4 h fast beginning at lights-on. To determine glucose tolerance, mice were injected with sterilized 20% glucose solution (10 μl/g of body weight, i.p.). Blood glucose levels were measured before and 30, 60, 90 and 120 min after glucose injection.

At termination of the experiments, mice were euthanized by exsanguination under ketamine/xylazine anesthesia after a 4 h fast beginning shortly after lights-on. Blood was collected from the right ventricle with a 1 ml syringe fitted with a 20 gauge hypodermic

needle. Serum was separated by centrifugation and stored at −20°C. Tissues were excised, rinsed with PBS to remove blood, and snap frozen in liquid nitrogen. Liver, heart, and individual fat pats were dissected and weighed. Tissue samples were stored at −80°C. Additional tissue samples were immediately embedded in OCT, frozen on dry ice, and stored at −20°C or formalin fixed overnight and stored in 70% ethanol at 4°C until processing and histological analysis.

Histology

Tissue was processed in a dehydrating ethanol gradient followed by xylene incubation and paraffin embedding. Paraffin blocks of tissue were cut into sections of 1 to 3 μm thickness and stained for hematoxylin and eosin (H&E). Frozen sections were cut at 10 μm thickness and subjected to Oil-Red-O staining.

Lipid analysis

Total lipids from liver and adipose were analyzed as previously described (15). Hepatic cholesterol and triglycerides were determined using enzymatic, colorometric assays. For GC/MS, total lipid extracts were saponified and esterified with 10% boron trifluoride in methanol (BF3-methanol 10%; Supelco, Bellefonte, PA). BF_3 and methanol were removed, and samples were injected into a gas chromatography system (6890 GC G2579A system; Agilent, Palo Alto, CA) equipped with a split injection system with parallel OMEGA-WAX^{TM} 250 capillary columns (Supelco) and either an FID detector (quantitative) or Agilent 5973 network mass selective detector (target identity). The GC program was: injector: 1 μl at 10:1 spilit, 250°C; detector: FID, 260°C; oven: 160°C (5 min) to 220°C at 4°C/min; carrier: helium, 1.2 ml/min. Hepatic levels of diacylglycerol and ceramide were determined as previously described (19, 20).

The acyl-carnitine extraction method is a modification of the method previously described (21). Tissues were weighed and homogenized in water and extracted with 80% acetonitrile with a series of vortexing, sonication, and centrifugation at 4000 rpm for 10 min. The supernatant was transferred into a vial, dried under nitrogen, and reconstituted with 100 μl of methanol. D3-C2, D3-C4, and D3-C16 acylcarnitines were used as internal standards for short- and long-chain acyl carnitines, respectively. Analyses of acylcarnitines was carried out using a Shimadzu UFLC coupled with an AB Sciex 4000-Qtrap hybrid linear ion trap triple quadrupole mass spectrometer in multiple reaction monitoring mode. Acyl carnitines were analyzed using an XTerra MS C8 3.5 μm, 3.0 × 100 mm column. The mobile phase consisted of 75/25 methanol/water, 0.5% formic acid + 0.1% ammonium formate as solvent A and 80% of (99/1 methanol/water, 0.5% formic acid + 0.1% ammonium formate): 20% chloroform as solvent B. For the analyses of acyl carnitines, the separation was achieved using a gradient of 0 to 100% solvent B in 10 min and maintaining at 100% B for the next 8 min. The column equilibrated back to the initial conditions in 3 min. The flow rate was 0.5 ml/min with a column temperature of 30°C. The sample injection volume was 10 uL. The mass spectrometer was operated in the positive electrospray ionization mode with optimal ion source settings determined by synthetic standards of acylcarnitines with a declustering potential of 86 V, entrance potential of 10 V, collision energy of 53 V, collision cell exit potential of 6 V, curtain gas of 20 psi, ion spray voltage of 5500 V, ion source gas1/gas2 of 40 psi, and temperature of 550°C. Multiple species of acyl carnitines wewre quantitated by monitoring species specific precursor product ion pairs.

Enzyme assays

Fatty acid elongation was determined as described previously (22). Briefly, microsomes (30 μg total protein) were incubated in a reaction mixture containing 150 μM [^{14}C] malonyl-CoA (American Radiolabeled Chemicals, Inc., St. Louis, MO) and 20 μM of the indicated fatty acids in the presence of 100 μM CoA, 1 mM ATP, and 1 mM NADPH at 37°C for 10 min. Fatty acids were extracted from the reaction mixture, and the total incorporation of [^{14}C] malonyl-CoA to fatty acid substrates was measured by scintillation counting.

Stearoyl CoA desaturase (SCD) activity was determined by measuring the amount of [1-^{14}C] oleic acid generated from [1-^{14}C] stearic acid as previously described (23, 24). The reaction medium contained 4 mM ATP, 100 μM CoA, 1.25 mM NADH, 500 μM nicotinamide, 5 mM $MgCl_2$, 64 mM NaF, 1.5 mM glutathione, 64 mM potassium phosphate (pH 7.2), and 100 μM [1-^{14}C] stearic acid (6650 dpm/nmol) as a BSA emulsion with a total reaction volume of 500 μl. The reaction was initiated by adding 0.3 mg mouse hepatic microsomes into the reaction medium. After incubation at 37°C in a water bath for 10 min, the reaction was stopped by adding 0.5 ml of 5 M potassium hydroxide in 10% methanol. Lipids were saponified, extracted with Folch reagent (chloroform/methanol 2:1 + 0.01% BHT (v/v/w), and dried under streaming nitrogen gas. Lipids were methylated in 1 ml of 14% BF3/methanol overnight at 55°C. Lipid esters were reextracted in 2 ml of chloroform, washed with 1 ml of water, and dried under nitrogen. Samples were loaded onto 10% argentinated TLC plates (#310496 56; Whatman, Piscataway, NJ). Plates were developed in hexane/diethyl ether (17:3, v/v), and radioactivity was measured by phosporimaging on a Typhoon FLA9000 Imaging System. SCD activity was expressed as nmol of oleate formed from stearate C18:0 per mg microsomal protein per hour.

Protein and RNA analysis

Membrane proteins were prepared and analyzed by SDS-PAGE and immunoblot analysis as previously described (25). The isolation of total RNA and the determination of relative transcript abundance by quantitative real-time PCR for both tissues and cells was conducted as previously described (25).

Statistical analysis

Body composition data were analyzed by two-way repeated measures ANOVA. Bonferroni posts tests were used where indicated. Comparisons between genotypes for other measures were conducted with two-tailed *t*-tests. All statistical analyses were conducted using GraphPad Prism statistical analysis software.

RESULTS

D2 deficient mice are susceptible to EA-induced obesity, dyslipidemia, and loss of glycemic control

To determine the role of D2 in the metabolism of dietary EA, mice were challenged with an EA-enriched diet for 8 weeks beginning at 8 weeks of age. As previously reported, differences in body weight, body composition, and other measures of obesity and lipid metabolism were not observed at the initiation of the study (Fig. 1, Reference 15). After EA feeding, we observed a modest but significant increase in body weight in D2 KO mice compared with wild-type controls. Analysis of body composition by MRI indicated a significant increase in fat mass in D2 KO mice after 8 weeks on diet. The accumulation of excess adipose tissue occurred primarily in epididymal and retroperitoneal depots (**Fig. 1B**). Whereas lean mass increased in wild-type mice during EA feeding, it remained relatively constant in D2 KO and was significantly lower than in wild-type controls at the termination of the study (Fig. 1A). The

expansion of adipose mass in the absence of an increase in lean mass resulted in a substantial increase in adiposity in D2 KO mice (Fig. 1C). Histological analysis of epididymal fat indicates that the expansion of adipose tissue was associated with the enlargement of adipocytes (Fig. 1D). Fasting glucose levels were increased in D2 KO mice compared with wild-type controls (Fig. 1E). A glucose tolerance test conducted after 7 weeks on diet revealed a decrease in glucose disposal consistent with the development of insulin resistance (Fig. 1F, G). Whereas fasting levels of triglycerides were unaffected, serum cholesterol was significantly elevated (**Table 1**).

The expansion of adipose and the loss of glycemic control are generally associated with adipose tissue inflammation. Consistent with the expansion of adipose tissue, leptin levels were elevated in D2 KO mice (Table 1). However, we failed to detect any differences in other adipocytokines typically associated with inflammation. We also stained adipose tissue sections for CD68 and did not observe an accumulation of macrophages or the presence of crown-like structures (data not shown). These data suggest the absence of inflammation in D2 KO adipose tissue after EA feeding despite the increase in adipose mass and adipocyte hypertrophy.

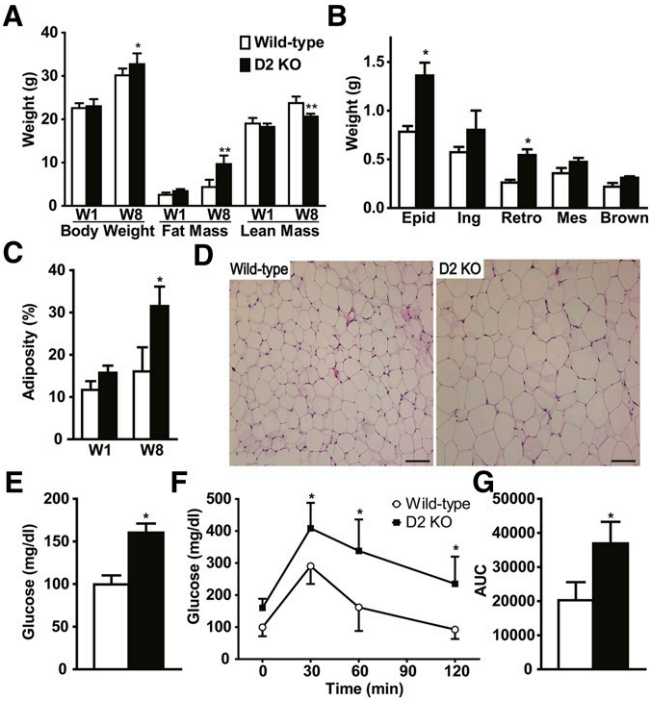

Fig. 1. Dietary erucic acid promotes obesity and loss of glycemic control in D2 KO mice. A: Body weight and composition were measured by MRI before (W1) and after 8 weeks (W8) of EA diet. B: Fat pads were dissected and weighed at the termination of the study. C: Adiposity was calculated by the ratio of fat mass to body weight. D: H&E staining of paraffin embedded epididymal fat. E: Fasting glucose levels at the termination of the study. F, G: A glucose tolerance test was performed at week 7, and the area under each curve (AUC) was calculated. Data are mean ± SD (n = 7). A, C, F: Two-way, repeated measures ANOVAs were used to determine differences due to genotype and time. Bonferroni multiple comparisons between genotypes were conducted within each time point. Remaining comparisons were made using an unpaired *t*-test. $*P < 0.05$; $**P < 0.01$. Epid, epididymal; Ing, inguinal; Mes, mesenteric; Retro, retroperitoneal.

TABLE 1. Serum lipid and adipokine levels in wild-type and D2 KO mice after an EA-enriched diet

	Wild-type	D2 KO
Triglycerides (mg/dl)	24.5 ± 2.8	23.8 ± 3.0
Cholesterol (mg/dl)	67.05 ± 6.036	125.7 ± 6.5 *
Leptin (ng/ml)	2.70 ± 1.18	20.24 ± 6.53 *
IL-6 (pg/ml)	7.99 ± 0.89	10.30 ± 2.31
Resistin (pg/ml)	2991 ± 187	2,570 ± 245
TNF-α (pg/ml)	3,104 ± 276	2,806 ± 348
PAI-1 (pg/ml)	3,104 ± 276	2,806 ± 348
Insulin (ng/ml)	0.30 ± 0.06	0.299 ± 0.13

D2 does not influence the development of diet-induced obesity

D2 is up-regulated in liver of obese and insulin-resistant mice, suggesting that D2 might modulate the development of obesity phenotypes in multiple mouse models (26) (Supplementary Figure I). First, mice were challenged with a HF (45% kCal) diet for 12 weeks beginning at 8 weeks of age (**Fig. 2**). Although there was a modest increase in fat mass, we observed no differences in body weight, adiposity, fasting glucose, or glucose tolerance. There were also no differences in food intake or blood lipids (Supplementary Table III). We next crossed D2 deficient mice with the leptin-deficient (ob/ob) strain, maintained them on standard rodent chow, and evaluated them at 8, 12, and 16 weeks of age. As in HF feeding, there was a tendency toward increased fat mass at 12 weeks, but there were no differences in other measures of obesity phenotypes (Supplementary Figure II, Supplementary Table III).

Dietary EA alters adipose fatty acid profile and gene expression

GC-MS analysis of the fatty acid profile in epididymal adipose showed that the relative abundance of EA was similar in wild-type and D2 KO mice and comprised less than 7% of the total fatty acids within adipose tissue (**Fig. 3**). The relative abundance of C18 and C20 MUFA was lower in D2 deficient mice and offset by an increase in C14 and C16 SFAs. The reduction in 20:1 and 18:1 in D2 KO mice is consistent with a reduction in β-oxidation and shortening of dietary EA before storage in adipose tissue triglycerides (TGs). However, given the increase in adipose tissue mass, the total amount of all fatty acids within adipose is greater in D2 KO than in wild-type mice. On the whole, there was an increase in SFAs and a decrease in MUFAs in adipose tissue, whereas the levels of PUFA were unaffected (Fig. 3, inset). These data are consistent with previous reports indicating that EA is not a preferred substrate for TG synthesis in adipose tissue (27).

To explore potential mechanisms for increased adiposity, we analyzed mRNA levels of key genes involved in the regulation of adipose function and lipid and carbohydrate metabolism. Insulin-induced gene-1 (INSIG1), but not INSIG2, was down-regulated in D2 KO mice. Although the expression of SREBP1 was not altered, several SREBP1 target

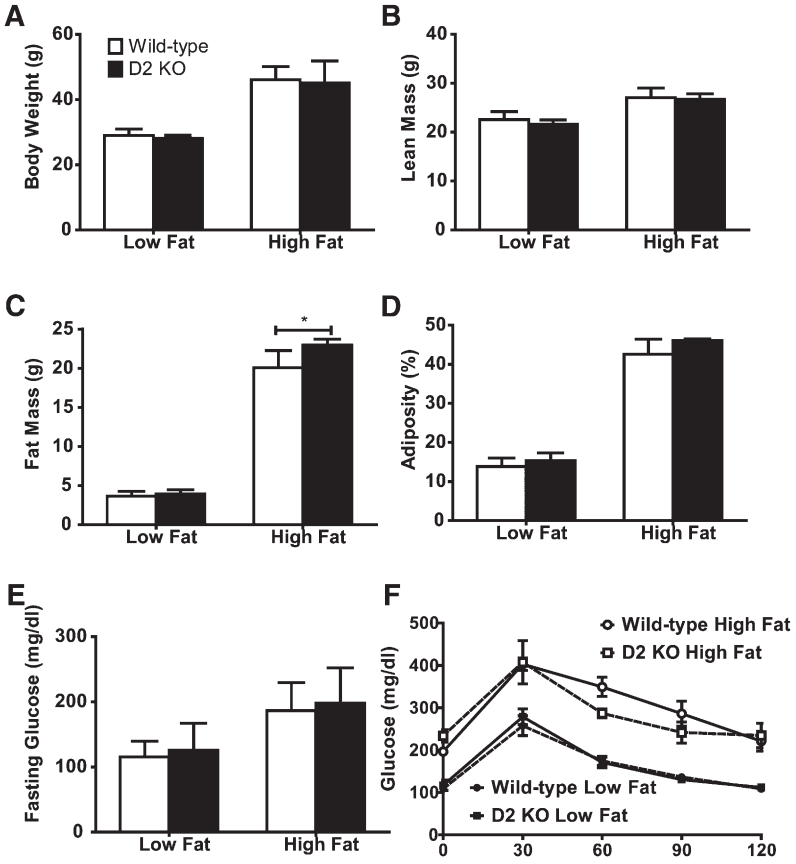

Fig. 2. D2 deficiency does not influence the development of diet-induced obesity. Wild-type and D2 KO mice were challenged with LF and HF diets for 12 weeks beginning at 8 weeks of age. Body weight (A), lean mass (B), fat mass (C), adiposity (D), fasting glucose (E), and glucose tolerance (F) were determined at the termination of the study. Data are mean ± SD (n = 10–13). Two-way ANOVAs were used to determine differences due to genotype and diet. Bonferroni multiple comparisons between genotypes were conducted within a diet to determine effects of genotype within each time point. $*P < 0.01$.

genes were down-regulated in adipose tissue of D2 KO mice fed EA, including acetyl-CoA carboxylase (ACC1), FAS, and stearoyl CoA-desaturase (SCD1) (Fig. 3B). There was also a 2.5-fold increase in the expression of D1 in adipose of D2 KO mice fed EA, but D1 expression in adipose is near the limit of detection in adipocytes (15). Transcription factors that regulate cholesterol, fatty acid, and glucose homeostasis were down-regulated in D2 KO mice (LXR, ChREBP) (Supplementary Figure III). These data are largely consistent with the development of insulin resistance in adipose tissue associated with adipocyte hypertrophy, suggesting these changes are reflective of the development of the obesity and insulin resistance rather than mechanisms for EA-dependent phenotypes in D2 KO mice.

EA promotes hepatic steatosis in D2 deficient mice

The development of obesity and adipose insulin resistance is associated with ectopic lipid accumulation. H&E staining of liver sections revealed vacuolar structures that stained positively with Oil-Red-O in D2 KO mice (**Fig. 4**). Hepatic triglycerides and cholesterol were elevated in the D2 KO mice compared with controls. Whereas the alteration in the fatty acid profile in adipose tissue was limited to a few specific fatty acids, the hepatic fatty acid profile revealed significant differences for many fatty acid species. There is dramatic shift from wild-type to D2 KO mice toward more MUFAs (C18–C22) and fewer PUFAs (C18–C22) (Fig. 4E). The relative levels of DHA and AA, key inhibitors of hepatic lipogenesis that suppress SREBP1 processing and transcriptional activity, are significantly reduced.

EA is an inhibitor of fatty acid elongation, an essential step in PUFA synthesis (28). The deletion of fatty acid elongase 5 (ELOVL5) reduces hepatic levels of DHA and AA and promotes steatosis in mice (22). Therefore, we measured elongation of several ELOVL5 substrates to determine if EA reduced the activity of this enzyme in D2 KO mice (**Fig. 5**). Rather than causing a reduction in ELOVL5 activity, the elongation of intermediates of PUFA synthesis was significantly elevated. We next measured the abundance of mRNAs for lipogenic genes (Fig. 5B). Although mRNA for SREBP1 was elevated, we did not observe significant increases in key lipogenic genes, including ACC1 and FAS. There was a modest but significant increase in SCD1 mRNA, but there was no increase in enzyme activity (Fig. 5C). These data indicate that hepatic steatosis is unrelated to the relative reduction in PUFAs and disinhibition of hepatic SREBP1 processing and activity. Unlike adipose, there was no increase in hepatic expression of D1 in D2 KO liver.

The accumulation of diacylglycerol and ceramide is associated with the development of steatosis and the progression of NAFLD (29). Total diacylglycerols and ceramides appear to be elevated in hepatic lipid extracts from D2 KO mice. However, the levels were quite variable, and these differences did not reach statistical significance (Supplementary Figure V).

In contrast to adipose, where tissue mass is comprised almost exclusively of TGs, liver fatty acid profiles differ substantially from fatty acid content. When reported on a per gram tissue basis, the fatty acids that accumulate in liver are limited to EA and its chain-shortened products of peroxisomal metabolism (20:1, 18:1, and 16:1) (**Fig. 6**).

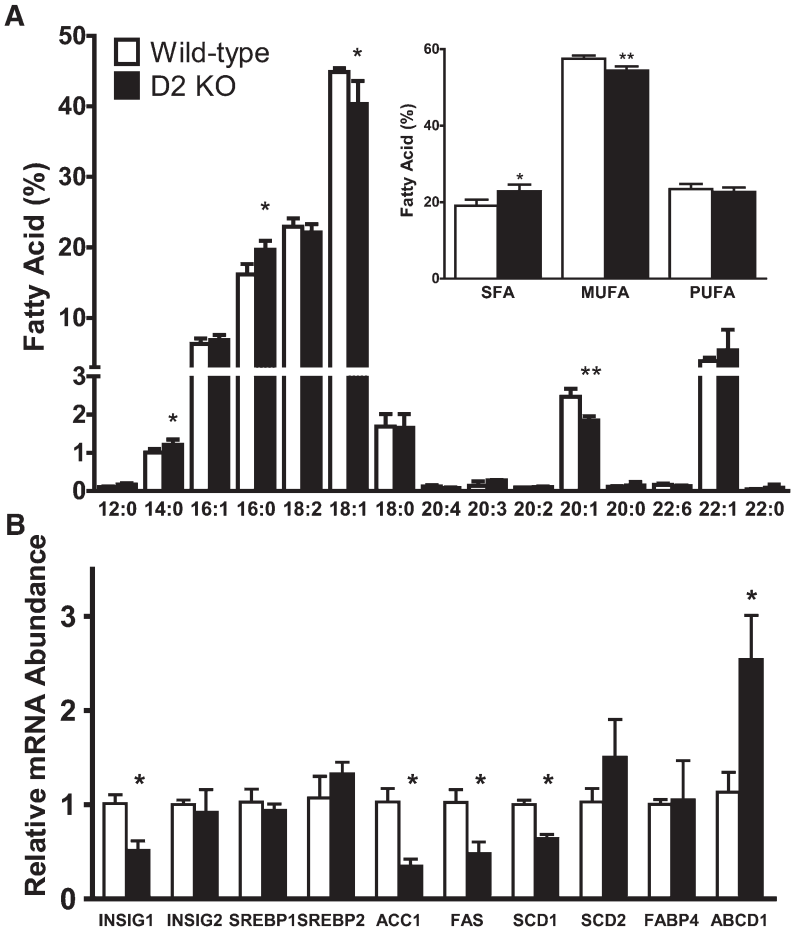

Fig. 3. Dietary EA alters adipose fatty acid profile and gene expression in D2 KO mice. A: Fatty acid profiles in total lipid extracts from epididymal fat pads were determined by GC-MS. Relative signal intensities were normalized to an internal standard (C17:0) and expressed as percentage of total fatty acids. Inset: Sum percentage of fatty acids by degree of saturation. B: The relative abundance of mRNAs for lipogenic regulators and enzymes was measured by qRT-PCR. Data are shown as mean ± SD (n = 7). Comparisons between genotypes for individual fatty acids and mRNAs were made using an unpaired *t*-test. $*P < 0.05$; $**P < 0.01$.

There is also an increase in 14-18 carbon SFA. Consequently, there is an accumulation of SFA and MUFA in the absence of any change in PUFA (Fig. 6, inset). Additional analysis of gene expression in liver revealed reductions in UCP2 and malic enzyme but no alterations in the expression of transcriptional regulators of sterol and carbohydrate metabolism or fatty acid modifying enzymes (Supplementary Figure IV). Collectively, the data suggest that the increase in hepatic MUFA is a consequence of peroxisomal shortening of EA. The increase in SFA does not appear to be a consequence of elevated lipogenesis and is more likely due to substrate competition for incorporation into secreted lipoproteins and mitochondrial oxidation.

DISCUSSION

The present study reveals a novel role for D2 in opposing disturbances in lipid metabolism associated with dietary EA. EA causes a transient lipidosis and dilated cardiomyopathy in several species and is associated with an elevation in hepatic triglycerides after long-term feeding in rats (30). However, mice are resistant to these effects. Although the absence of D2 sensitizes mice to EA feeding, the phenotype differs substantially from rats. We did not observe hypertriglyceridemia in the present study or in previous studies with an acute challenge (15). We also saw no evidence of cardiomyopathy. Nonetheless, dietary EA resulted in a robust disruption of lipid metabolism leading to an expansion of adipose tissue, the loss of glycemic control, and steatosis. This suggests that mice have sufficient D2 present at all times or can rapidly up-regulate D2 to compensate for the presence of EA in the diet.

D2 is an SREBP1 target gene and is up-regulated during adipogenesis, suggesting that D2 dependent peroxisomal metabolism may play an essential role in lipogenesis and TG storage. Indeed, an alternative pathway involving peroxisomal dihydroxyacetone phosphate acyltransferase accounts for approximately 40% of TG synthesis in 3T3-L1 cells (31). Although D2 may supply this pathway with fatty acyl-CoAs, the absence of D2 did not reduce lipid accumulation in mouse embryonic fibroblasts differentiated into adipocytes (15). Likewise, we observed no reduction in adipose mass in mouse models of diet-induced obesity regardless of whether adipose expansion was driven by excess dietary fat or by hyperphagia and lipogenesis. Consequently, the functional significance of SREBP1 regulated D2 expression remains unclear.

Although D2 opposes the accumulation of EA in adipose tissue and plasma after an acute dietary challenge (15), EA levels in wild-type and D2 KO mice did not differ after 8 weeks of EA feeding. Despite the fact that EA constituted 50% of the dietary fatty acid species, it accounts for only 5% of the fatty acids in adipose and did not differ between genotypes. This is in keeping with previous reports indicating

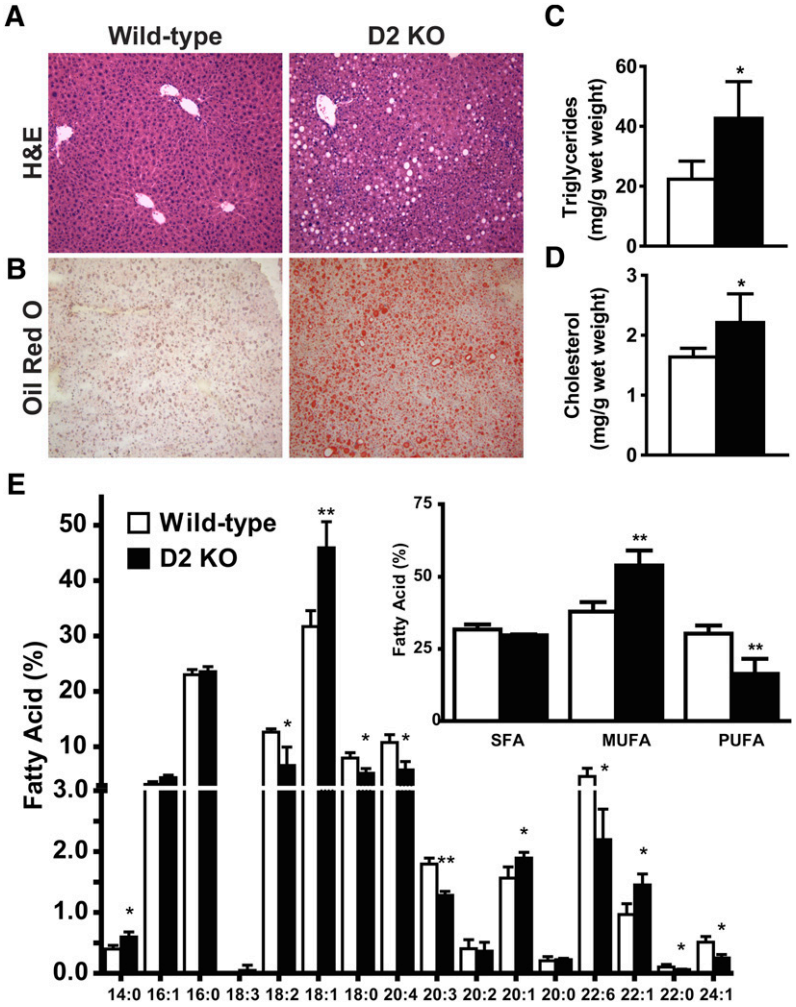

Fig. 4. Dietary EA promotes hepatic steatosis and alters fatty acid profile in D2 KO mice. A, B: Liver sections from wild-type and D2 KO mice were stained with H&E and for neutral lipids with Oil Red O. C, D: Total triglycerides and cholesterol in hepatic tissue were determined using colorimetric assays. E: Fatty acid profiles of total hepatic lipids were measured by GC-MS. Fatty acid levels were normalized to an internal standard (C17) and expressed as percentage of total fatty acids. Inset: Sum percentage of fatty acids by degree of saturation. Data are shown as mean ± SD (n = 7). Comparisons between genotypes were made using an unpaired *t*-test. $*P < 0.05$; $**P < 0.01$.

that EA is a poor substrate for esterification and storage as TG and suggests that EA incorporation into adipose TGs reaches its maximum irrespective of the presence or absence of D2 (27). In the presence of D2, EA is likely shortened to 16- and 18-carbon MUFAs in peroxisomes. Indeed, these are elevated in the adipose tissue of wild-type compared with D2 KO mice. If not stored as EA in the adipose TG pool and not metabolized to shorter chain MUFAs, dietary EA must be metabolized outside of adipose tissue.

As in adipose tissue, the levels of EA are quite low in the liver and constitute less than 2% of the fatty acid profile. However, there is a significant increase in EA in D2 KO mice, as well as 16-, 18-, and 20-carbon MUFAs. The relatively small amount of hepatic EA and the accumulation of its chain-shortened metabolites suggest that EA is metabolized by peroxisomes in the liver. In contrast to adipose tissue, the liver expresses relatively low levels of D2 and high levels of D1 (9, 15). D1 is the closest family member to D2, and, although the transporters have distinct substrate spectra, there is significant overlap, including EA. D1 expression was increased in adipose of D2 KO mice fed EA but was unchanged in liver. This transporter may therefore compensate for the absence of D2 with respect to EA metabolism. Although the compensatory pathway prevents the accumulation of EA, it fails to prevent its disruptive effects on lipid metabolism.

The synthesis of 20- and 22-carbon PUFAs requires the activity of fatty acid elongases. In the absence of ELOVL5, mice develop steatosis due to PUFA deficiency (22). EA inhibits fatty acid elongation and is used clinically to reduce VLCFAs in ALD patients, suggesting this could be a mechanism for EA-mediated disruptions in lipid metabolism in the absence of D2. Indeed, there is a relative reduction in hepatic PUFAs, including DHA and AA in D2 KO mice (Fig. 4). However, fatty acid elongase activity was elevated in microsomes isolated from D2 KO mice. This increase in activity also appears to be the case in vivo based on the increase in 20:3ω3, the product of 18:3ω3 elongation. Consequently, the relative decline in PUFAs in the fatty acid profile may be misleading. There was no reduction in the absolute levels of PUFAs in the liver of D2 KO mice (Fig. 6), but whether the absolute or relative levels of PUFAs is critical to feedback inhibition of lipogenesis is not known. The expression of lipogenic genes was largely unaffected, and there was no increase in the activity of SCD1, an essential enzyme for TG storage. These data suggest that hepatic PUFA content rather than relative levels are important for regulation of SREBP1 activity in vivo.

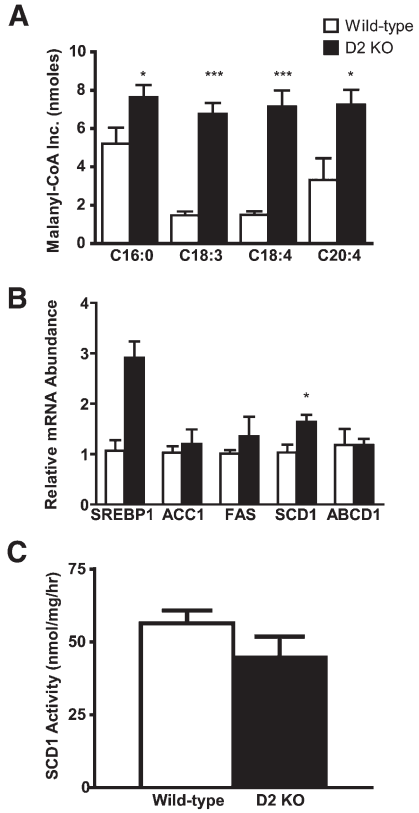

Fig. 5. Dietary EA increases elongase activity but has no effect on lipogenic genes or SDC1 activity. A: Elongation of fatty acids in liver microsomes was determined by incorporation of malonyl CoA into the indicated fatty acid substrates. B: mRNA levels of liver lipogenic genes were measured by qRT-PCR. C: Activity of stearoyl-CoA desaturase was determined by conversion of labeled stearate to oleate in isolated liver microsomes. Data are shown as mean ± SD (n = 4). Comparisons between genotypes were made using an unpaired *t*-test. $*P < 0.05$; $**P < 0.01$; $***P < 0.001$.

A surprising observation is that expansion of the adipose tissue and loss of glycemic control was not associated with the accumulation of inflammatory cytokines in plasma. Similarly, there was no evidence for macrophage infiltration and the formation of crown-like structures in adipose tissue. One potential explanation is that the feeding period for the present experiment was only 8 weeks. Perhaps with increased time, these hallmarks of obesity and insulin resistance would have presented. Regardless, the data indicate that adipose dysfunction and inflammation was not causative in the EA-dependent phenotype in D2 KO mice.

The role of peroxisomal metabolism in the development of obesity phenotypes is poorly understood but may play a significant role. A recent study indicates that D2 expression and hepatic peroxisomal metabolism are increased during the development of obesity and insulin resistance in HF fed mice (26). The products of peroxisomal metabolism include acylcarnitines that are capable of bypassing carnitine palmitoyltransferase 1 for entry into mitochondria irrespective of cellular levels of malonyl-CoA. HF feeding and excess caloric intake result in mitochondrial overload, incomplete β-oxidation, and the accumulation of medium-chain acylcarnitines in the plasma of rodents (32). Therefore, peroxisomal β-oxidation could potentially contribute to mitochondrial overload and promote obesity phenotypes after HF feeding. We measured acylcarnitines in liver of wild-type and D2 KO mice but did not observe differences in individual acylcarnitines or the sums of short-, medium-, or long-chain species (Supplementary Figure VI).

Conversely, there is an increase in peroxisomal lipid metabolism in mice resistant (A/J) to obesity and steatosis after HF feeding, suggesting that peroxisomes may play a protective role with respect to the development of obesity phenotypes (33). We have confirmed an increase in hepatic expression of D2 after HF feeding and have also observed an increase in ob/ob mice (Supplementary Figure I). However, the absence of D2 played neither a protective nor a deleterious role in the development of obesity phenotypes in mouse models of obesity and insulin resistance. Although there may be a role for peroxisomes in the development of obesity and steatosis, it is independent of the presence or absence of D2 unless mice are challenged with a diet containing EA and perhaps other fatty acids that require peroxisomal metabolism before storage in TG pools.

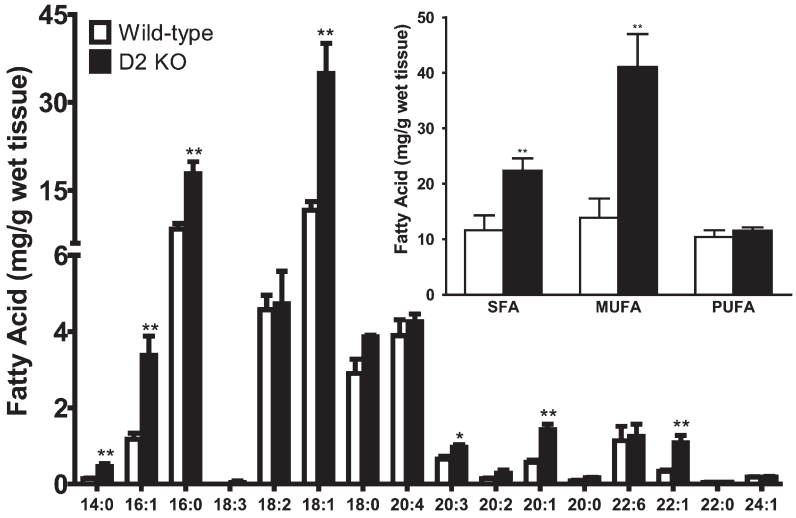

Fig. 6. Hepatic fatty acid content after EA feeding in wild-type and D2 KO mice. Fatty acid content (mg/g tissue) in total hepatic lipids was measured by GC-MS. Inset: Sum of fatty acid content by degree of saturation. Data are shown as mean ± SD (n = 7). Comparisons between genotypes were made using an unpaired *t*-test. $*P < 0.05$; $**P < 0.01$.

The key finding from this study is that D2 opposes disturbances in lipid metabolism caused by dietary EA. The abundance of D2 in adipose tissue is 50-fold higher than in liver, suggesting that metabolism of EA allows for its incorporation into TG within adipose tissue. In the absence of D2, EA is metabolized to its chain-shortened metabolites in liver. The result is a substantial increase in hepatic MUFA derived from peroxisomes as opposed to biosynthetic or endocytic sources. This additional source of MUFA is incorporated into hepatic TG and cholesterol esters but cannot suppress hepatic expression of lipogenic genes. Consequently, there is an expansion of adipose tissue, adipocyte hypertrophy, loss of glycemic control, and the development of steatosis. These observations reveal essential roles for D2 and peroxisomes in metabolizing dietary lipids that require remodeling before storage in TG and opposing disruptions in lipid metabolism due to the failure to efficiently "trap" dietary fatty acids in adipose tissue.

REFERENCES

1. Wanders, R. J., and H. R. Waterham. 2006. Biochemistry of mammalian peroxisomes revisited. *Annu. Rev. Biochem.* **75:** 295–332.
2. Sprecher, H. 2000. Metabolism of highly unsaturated n-3 and n-6 fatty acids. *Biochim. Biophys. Acta.* **1486:** 219–231.
3. Su, H-M., A. B. Moser, H. W. Moser, and P. A. Watkins. 2001. Peroxisomal straight-chain Acyl-CoA oxidase and D-bifunctional protein are essential for the retroconversion step in docosahexaenoic acid synthesis. *J. Biol. Chem.* **276:** 38115–38120.
4. Coleman, R. A., T. M. Lewin, C. G. Van Horn, and M. R. Gonzalez-Baró. 2002. Do long-chain Acyl-CoA synthetases regulate fatty acid entry into synthetic versus degradative pathways? *J. Nutr.* **132:** 2123–2126.
5. Wanders, R. J., W. F. Visser, C. W. van Roermund, S. Kemp, and H. R. Waterham. 2007. The peroxisomal ABC transporter family. *Pflugers Arch.* **453:** 719–734.
6. Cappa, M., C. Bizzarri, C. Vollono, A. Petroni, and S. Banni. 2011. Adrenoleukodystrophy. *Endocr. Dev.* **20:** 149–160.
7. Ferrer, I., P. Aubourg, and A. Pujol. 2010. General aspects and neuropathology of X-linked adrenoleukodystrophy. *Brain Pathol.* **20:** 817–830.
8. Holzinger, A., S. Kammerer, J. Berger, and A. A. Roscher. 1997. cDNA cloning and mRNA expression of the human adrenoleukodystrophy related protein (ALDRP), a peroxisomal ABC transporter. *Biochem. Biophys. Res. Commun.* **239:** 261–264.
9. Berger, J., S. Albet, M. Bentejac, A. Netik, A. Holzinger, A. A. Roscher, M. Bugaut, and S. Forss-Petter. 1999. The four murine peroxisomal ABC-transporter genes differ in constitutive, inducible and developmental expression. *Eur. J. Biochem.* **265:** 719–727.
10. Pujol, A., I. Ferrer, C. Camps, E. Metzger, C. Hindelang, N. Callizot, M. Ruiz, T. Pampols, M. Giros, and J. L. Mandel. 2004. Functional overlap between ABCD1 (ALD) and ABCD2 (ALDR) transporters: a therapeutic target for X-adrenoleukodystrophy. *Hum. Mol. Genet.* **13:** 2997–3006.
11. Lombard-Platet, G., S. Savary, C. O. Sarde, J. L. Mandel, and G. Chimini. 1996. A close relative of the adrenoleukodystrophy (ALD) gene codes for a peroxisomal protein with a specific expression pattern. *Proc. Natl. Acad. Sci. USA.* **93:** 1265–1269.
12. Fourcade, S., M. Ruiz, C. Camps, A. Schluter, S. M. Houten, P. A. Mooyer, T. Pampols, G. Dacremont, R. J. Wanders, M. Giros, et al. 2009. A key role for the peroxisomal ABCD2 transporter in fatty acid homeostasis. *Am. J. Physiol. Endocrinol. Metab.* **296:** E211–E221.
13. van Roermund, C. W., W. F. Visser, L. Ijlst, A. van Cruchten, M. Boek, W. Kulik, H. R. Waterham, and R. J. Wanders. 2008. The human peroxisomal ABC half transporter ALDP functions as a homodimer and accepts acyl-CoA esters. *FASEB J.* **22:** 4201–4208.
14. van Roermund, C. W. T., W. F. Visser, L. Ijlst, H. R. Waterham, and R. J. A. Wanders. 2011. Differential substrate specificities of human ABCD1 and ABCD2 in peroxisomal fatty acid [beta]-oxidation.*Biochim. Biophys. Acta.* **1811:** 148–152.
15. Liu, J., N. S. Sabeva, S. Bhatnagar, X. A. Li, A. Pujol, and G. A. Graf. 2010. ABCD2 is abundant in adipose tissue and opposes the accumulation of dietary erucic acid (C22:1) in fat. *J. Lipid Res.* **51:** 162–168.
16. Weinhofer, I., M. Kunze, H. Rampler, A. L. Bookout, S. Forss-Petter, and J. Berger. 2005. Liver X receptor alpha interferes with SREBP1c-mediated Abcd2 expression. Novel cross-talk in gene regulation. *J. Biol. Chem.* **280:** 41243–41251.
17. Bremer, J., and K. R. Norum. 1982. Metabolism of very long-chain monounsaturated fatty acids (22:1) and the adaptation to their presence in the diet. *J. Lipid Res.* **23:** 243–256.
18. Ferrer, I., J. Kapfhammer, C. Hindelang, S. Kemp, N. Troffer-Charlier, V. Broccoli, N. Callyzot, P. Mooyer, J. Selhorst, P. Vreken, et al. 2005. Inactivation of the peroxisomal ABCD2 transporter in the mouse leads to late-onset ataxia involving mitochondria, Golgi and endoplasmatic reticulum damage. *Hum. Mol. Genet.***214:** 3565–3577.
19. Sumanasekera, C., O. Kelemen, M. Beullens, B. E. Aubol, J. A. Adams, M. Sunkara, A. Morris, M. Bollen, A. Andreadis, and S. Stamm. 2011. C6 pyridinium ceramide influences alternative pre-mRNA splicing by inhibiting protein phosphatase-1. *Nucleic Acids Res.* In press.
20. Ren, H., L. Federico, H. Huang, M. Sunkara, T. Drennan, M. A. Frohman, S. S. Smyth, and A. J. Morris. 2010. A phosphatidic acid binding/nuclear localization motif determines lipin1 function in lipid metabolism and adipogenesis. *Mol. Biol. Cell.* **21:** 3171–3181.
21. van Vlies, N., L. Tian, H. Overmars, A. H. Bootsma, W. Kulik, R. J. Wanders, P. A. Wood, and F. M. Vaz. 2005. Characterization of carnitine and fatty acid metabolism in the long-chain acyl-CoA dehydrogenase-deficient mouse. *Biochem. J.* **387:** 185–193.
22. Moon, Y-A., R. E. Hammer, and J. D. Horton. 2009. Deletion of ELOVL5 leads to fatty liver through activation of SREBP-1c in mice. *J. Lipid Res.* **50:** 412–423.
23. Garg, M. L., A. B. Thomson, and M. T. Clandinin. 1988. Effect of dietary cholesterol and/or omega 3 fatty acids on lipid composition and delta 5-desaturase activity of rat liver microsomes. *J. Nutr.* **118:** 661–668.
24. Garg, M. L., A. A. Wierzbicki, A. B. Thomson, and M. T. Clandinin. 1988. Dietary cholesterol and/or n-3 fatty acid modulate delta 9-desaturase activity in rat liver microsomes. *Biochim. Biophys. Acta.* **962:** 330–336.
25. Sabeva, N. S., E. J. Rouse, and G. A. Graf. 2007. Defects in the leptin axis reduce abundance of the ABCG5-ABCG8 sterol transporter in liver. *J. Biol. Chem.* **282:** 22397–22405.
26. Kozawa, S., A. Honda, N. Kajiwara, Y. Takemoto, T. Nagase, H. Nikami, Y. Okano, S. Nakashima, and N. Shimozawa. 2011. Induction of peroxisomal lipid metabolism in mice fed a high-fat diet. *Mol. Med. Report.* **4**: 1157–1162.
27. Christophersen, B., T. Krogstad, and J. Norseth. 1983. Metabolism of erucic acid in adipocytes isolated from rat epididymal fat. *Lipids.* **18:** 137–141.
28. Koike, R., S. Tsuji, T. Ohno, Y. Suzuki, T. Orii, and T. Miyatake. 1991. Physiological significance of fatty acid elongation system in adrenoleukodystrophy. *J. Neurol. Sci.* **103:** 188–194.
29. Nagle, C. A., E. L. Klett, and R. A. Coleman. 2009. Hepatic triacylglycerol accumulation and insulin resistance. *J. Lipid Res.* **50(Suppl):** S74–S79.
30. Abdellatif, A. M., and R. O. Vles. 1970. Pathological effects of dietary rapeseed oil in rats. *Nutr. Metab.* **12:** 285–295.
31. Hajra, A. K., L. K. Larkins, A. K. Das, N. Hemati, R. L. Erickson, and O. A. MacDougald. 2000. Induction of the peroxisomal glycerolipid-synthesizing enzymes during differentiation of 3T3–L1 adipocytes. *J. Biol. Chem.* **275:** 9441–9446.
32. Koves, T. R., J. R. Ussher, R. C. Noland, D. Slentz, M. Mosedale, O. Ilkayeva, J. Bain, R. Stevens, J. R. B. Dyck, C. B. Newgard, et al. 2008. Mitochondrial overload and incomplete fatty acid oxidation contribute to skeletal muscle insulin resistance. *Cell Metab.* **7:** 45–56.
33. Hall, D., C. Poussin, V. R. Velagapudi, C. Empsen, M. Joffraud, J. S. Beckmann, A. E. Geerts, Y. Ravussin, M. Ibberson, M. Oresic, et al. 2010. Peroxisomal and microsomal lipid pathways associated with resistance to hepatic steatosis and reduced pro-inflammatory state. *J. Biol. Chem.* **285:** 31011–31023.